SOPHION BIOSCIENCE

Application Report

CHO-hNa$_V$1.7 assay on Qube pharmacology, biophysical characterization and the effect of internal fluoride

A robust assay with high reproducibility and accuracy, as well as high success rate and excellent control of $V_{½}$ over a long duration

Summary

Na$_V$1.7 has moved in the focus of the drug discovery industry in the last years as numerous studies provided strong proof for the efficacy to alleviate both neuropathic and inflammatory pain (Sun, Cohen, & Dehnhardt, 2014). We demonstrate high reproducibility and precision of Na$_V$1.7 data recorded on Qube.

- 95% of all tested cells had a GΩ seal in the beginning and 61% at the end of a long, 70 min experiment.
- $V_{1/2}$ is stable over time with only a slight shift
- Experiments can be performed in physiological ringers, however fluoride in the internal solution significantly increases success rate without any altering biophysical parameters.

Introduction and scope

The voltage-gated sodium channels (Na$_V$'s) play a critical role in electrical signal transduction as they are involved in the initiation and propagation of action potentials. In spite their apparent vital role, it has been proven possible to develop a spectrum of therapeutically effective drugs that target the channel whilst exhibiting only few side effects. Notably, all these drugs were discovered by employing empirical pharmacological techniques and Na$_V$ was only subsequently found to mediate the effect. However, development of more selective and more efficacious drugs against Na$_V$'s was hampered by the lack of an appropriate screening method that would allow the optimization of subtype selectivity. Nevertheless, Na$_V$ drug discovery has recently been reinvigorated driven by advances in the field of automated patch clamp. This technique allows for accurate investigation of Na$_V$ subtype-specific pharmacology (Clare JJ, Tate, SN, Nobbs, 2000).

Na$_V$1.7 is predominantly expressed in the peripheral nervous system (PNS), both in sensory and sympathetic neurons as well as in Schwann cells and neuroendocrine cells. Na$_V$1.7 belongs to the family of Tetrodotoxin (TTX) – sensitive Nav's and like all other members in this group, Na$_V$1.7 exhibits rapid activation and inactivation kinetics. Na$_V$1.7 is further characterized by its slow recovery from the inactivated state, a fact that enables Na$_V$1.7 – expressing cells to amplify slowly developing, sub-threshold depolarizing inputs. Recent studies have revealed Na$_V$1.7 as pivotal entity in mediating neuropathic and inflammatory pain (Savio-Galimberti, Gollob, & Darbar, 2012). Given its limited expression profile, Na$_V$1.7 was suggested as ideal target for analgesics.

Many Na$_V$ inhibitors preferentially inhibit gating states at depolarized membrane potentials (i.e. active and inactive state) over states at hyperpolarized potentials (closed or resting state). For cells that generate and propagate action potentials, state-dependence of drug inhibition gives often rise to a higher inhibition at higher frequencies of channel activation. This phenomenon is termed "use-dependent inhibition". Such a use-dependent inhibition is favorable for drug action as disease states often arise from hyperexcitability of the cell, hence, a use-dependent inhibitor is more potent on the malfunctioning cell as it is on the healthy.

In the present study, we highlight two commonly used voltage protocols to study state and use-dependence and verify the accuracy and robustness of Qube as a screening platform for drugs targeting Na$_V$1.7. In addition we evaluate the effect of fluoride in the internal solution as some scientists have raised concerns that this anion alters biophysical characteristics and thus provides false estimation of compound inhibition.

Results and discussion

Figure 1 shows the seal resistance (R_{seal}) of CHO-hNa_V1.7 cells measured on Qube at different time points throughout one experiment. The vast majority of cells showed a true gigaohm seal over the entire course of the experiment. To validate the assay, we assessed different biophysical parameters (Figure 2). A family of voltage steps from -140 mV to +70 mV in 10 mV increments elicited a transient current that reversed in agreement with the calculated reversal potential of Na^+ ($E_{rev}(Na^+)$ = +69 mV)(Figure 2A and B). The midpoint of steady-state fast inactivation ($V_{1/2}$) was -64 ± 2 mV (SD)(n = 89) and the apex of the activation IV (V_{min}) was -15 ± 3 mV (SD)(n = 89). Both values corresponded well with values reported in the literature (Mccormack et al., 2013).

As introduced above, many compounds targeting Na_V1.7 exhibit higher affinities towards either the activated or inactivated state than the closed state of the channel. IC_{50} values of these compounds critically depend on the frequency of voltage pulses or the holding potential (V_{hold}) from which the channel is stimulated. Therefore, to be able to determine correct IC_{50} values, it is imperative to have solid control of $V_{1/2}$ of inactivation over the entire course of the experiment. To assess stability of the $V_{1/2}$ value, we recorded inactivation curves over a 70 min duration in 4.3 min intervals (Figure 2D). $V_{1/2}$ remained almost constant over the first 30 min of the experiment and only a slight shift was observed in the further course. Furthermore, it has to be noted that a typical non-accumulated concentration response experiment does not exceed 20 min.

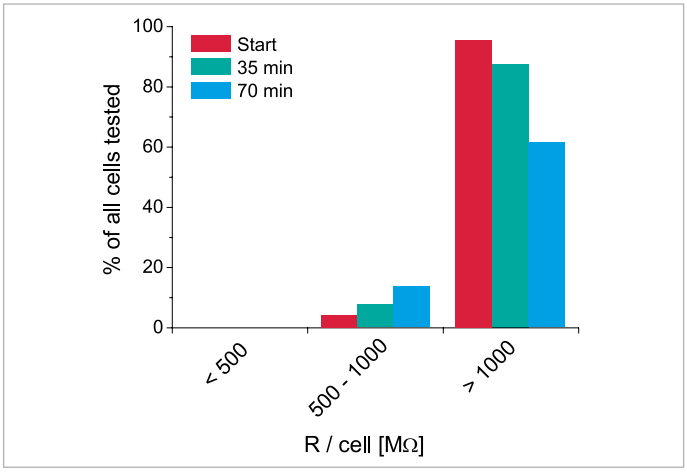

Fig. 1: Success rate measured as R_{seal} of CHO cells stably expressing Na_V1.7 recorded on Qube. Data is shown as % of all tested cells (96 cells). A multi hole chip with 10 holes was used for the experiment, thus, the recorded resistance value was multiplied by 10 to obtain the resistance value per cell.

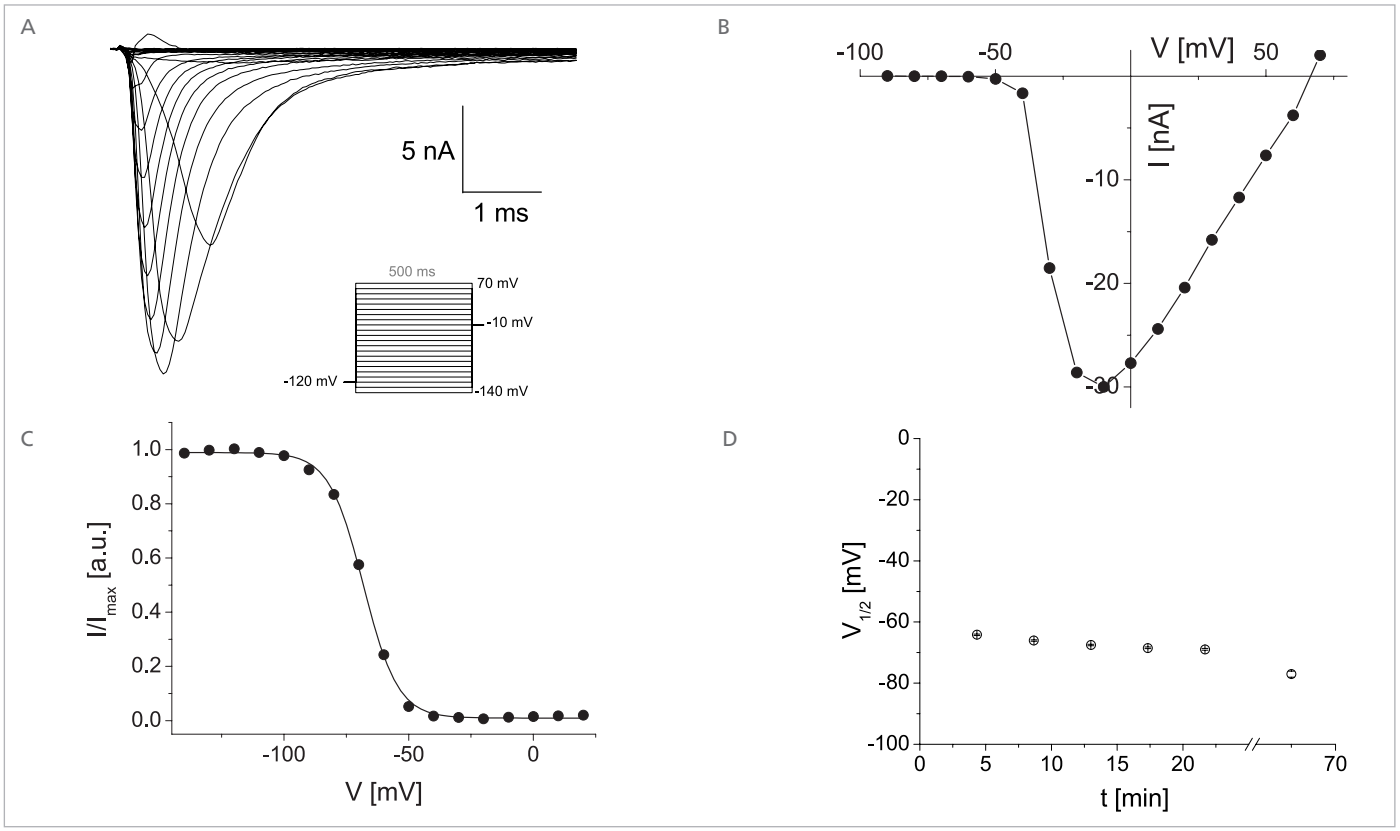

Fig. 2: hNa_V1.7 activation and inactivation curves. Data was recorded using Sophion`s standard solution composition with 140 mM F- in the internal solution. **A**: Representative current traces of a single well at different potentials. Currents were elicited using the voltage step protocol shown in the insert. The respective peak-current voltage relationship is shown in **B** (values from -140 to -90 were omitted). **C**: Inactivation curve determined as relative peak current at V = -10 mV with different voltage pre-pulses as indicated. The data was fitted using the Boltzmann equation **D**: Average $V_{1/2}$ values ± SD of n = 67 – 95 cells recorded over a long period of time.

In a next step, we tested the effect of different well-characterized inhibitors on $Na_V1.7$ using different voltage protocols. To assess use-dependent inhibition, we stimulated cells with a pulse train defined with 10 ms - long voltage pulses from V_{hold} = -120 mV to -10 mV every 100 ms and determined IC_{50} values at the first and the 10th pulse (Figure 3A). We found Amitriptyline to be two times more potent at the end of the 10 Hz pulse train than at the beginning. This is in line with earlier reports on Amitriptyline where a clear use-dependence of the compound was found (Cerne, Wakulchik, Li, Burris, & Priest, 2016). Another way of investigating the state-dependence of an inhibition is by keeping the channels at a partially inactivated state (e.g. close to $V_{1/2}$).

Using such a protocol, we found an even more pronounced inhibition of Amitriptyline on $Na_V1.7$ (Figure 3B). Importantly, no significant current run-down was observed in the DMSO control when held at $V_{1/2}$ for the entire duration of the experiment (Current change at the end of experiment = 104 ± 2% (n = 48)). Using the same approach, we further tested Tetracaine and TTX (Table 1). The obtained IC_{50} values correspond with values reported in the literature (Cerne et al., 2016; Zhang, Reichert, & Cohen, 2016). It is noted that the pore blocker TTX is devoid of use-dependency highlighting the need for electrophysiological measurements to detect such mode of action

[Table 1]: IC_{50} values of $Na_V1.7$ inhibitors determined using different voltage protocols as indicated.

	V_{hold} = 120 mV		V_{hold} = 65 mV
Compound	IC_{50} (10th Pulse)	IC_{50} (1st Pulse)	IC_{50} (10th Pulse)
Amitriptyline	2.1 µM	5.1µM	0.8 µM
Tetracain	21 µM	31.9 µM	3.8 µM
TTX	40 nM	50 nM	20 nM

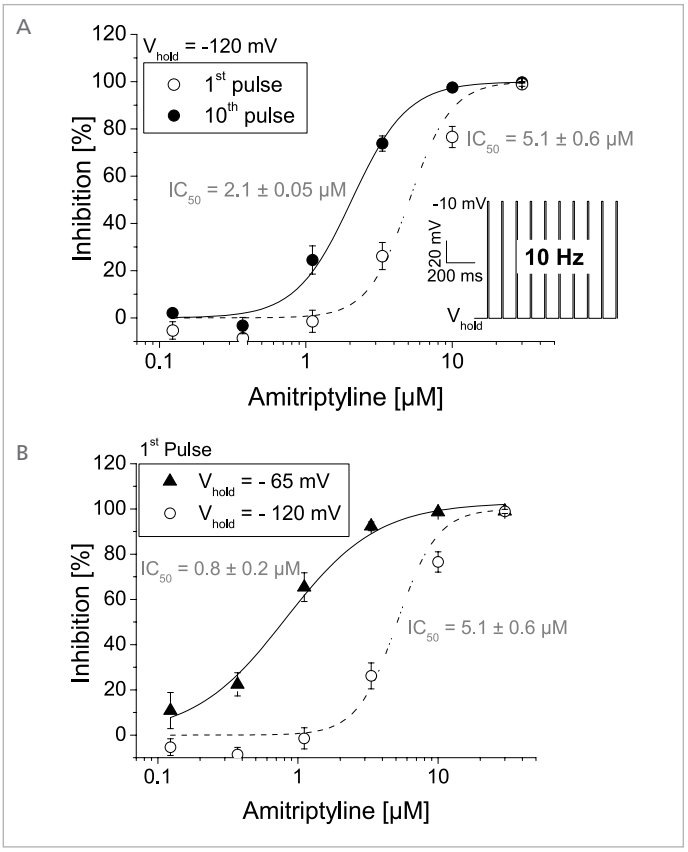

Fig. 3: Concentration response curve of Amitriptyline. Current was elicited using a pulse train protocol as shown in the insert. Following a baseline measurement, each cell was subjected to only one concentration (non-accumulated concentration response curve) and inhibition was calculated as Inhibition = ($I_{Amitriptyline}$ / $I_{Baseline}$)*100. In the same time frame, the change in current in the DMSO control was 104 ± 2% (n = 48). Data was fitted using the Hill equation and respective IC_{50} values are shown next to the curve. A: Use-dependent inhibition of Amitriptyline assessed at first and 10th pulse (n = 14-16 for each concentration). B: Inhibition of $Na_V1.7$ – mediated current from a partially-inactivated state (V_{hold} = -65 mV) and from the resting state (V_{hold} = -120 mV), here, inhibition was assessed at the first pulse. Shown data represents mean ± SD.

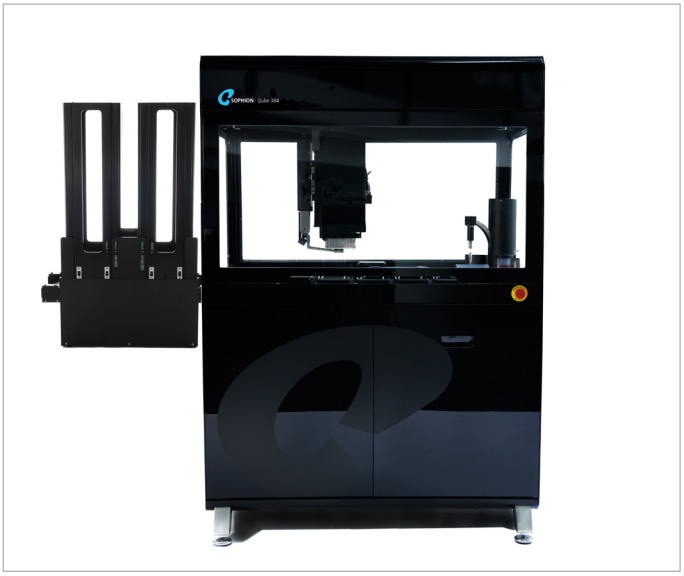

In a next set of experiments, we investigated the effect of internal fluoride on $Na_V1.7$ assay. Figure 4A shows the success rate over the duration of a long (> 1h) experiment. Success rate is defined as cells that passed the filer criteria that are: R/cell > 50 MΩ; persistent current at V = -30 and -10 mV < 100 pA/cell. Recordings with both 140 and 70 mM fluoride in the internal solution showed a high success rate that decreased only slightly throughout the 70 min of the experiment. This is also reflected in the true gigaohm seal over the entire course of the experiment (Figure 4B). Reducing internal fluoride concentration to 28 mM still showed a constantly high R_{seal} and thus success rate, however, a steady decrease in both parameters was observed after 20 min of experimentation. It was still possible to record $Na_V1.7$ currents using an intracellular solution devoid of fluoride but this significantly compromised success rate and stability of the assay. Biophysical parameters recorded in all four solutions corresponded with values reported in the literature (Table 2) (Mccormack et al., 2013), however, omitting fluoride resulted in a slightly larger variance of the data.

Table 2: Biophysical characteristics determined with various fluoride concentrations in the internal solution. Shown values are mean ± SD and were determined at the start of the experiment. 0 mM F- solution was further supplemented by 4 mM ATP.

	$V_{½}$ [mV]	V_{min} [mV]	n
0 mM F^-	-69 ± 3	-9 ± 3	62
28 mM F^-	-67 ± 2	-16 ± 2	87
70 mM F^-	-65 ± 2	-16 ± 2	91
140 mM F^-	-64 ± 2	-15 ± 2	95

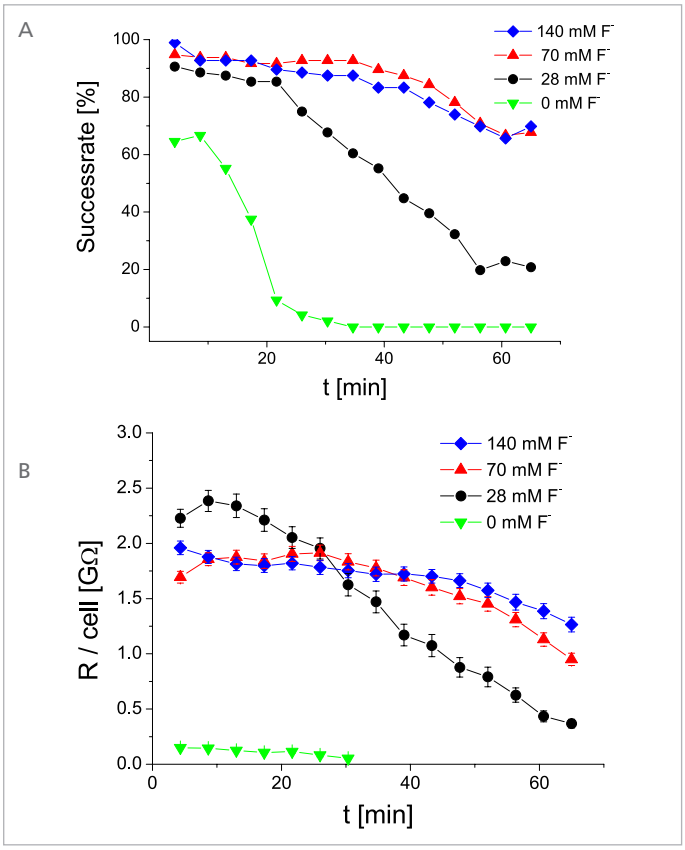

Fig. 4: Success rate (**A**) and R_{seal} (**B**) over time in various concentrations of internal fluoride as indicated. Success rate is defined as cells that passed the filter criteria (see text). Recordings were carried out using a 10 hole QChip, thus, measured resistances were 10 times lower as R/cell. Data in B represents mean ± s.e.m.

Materials and Methods

Cells Chinese hamster ovaria (CHO) cells stably expressing $hNa_V1.7$ (kindly provided by Anaxon) were grown and harvested according to Sophion`s standard procedure.

Solutions Standard external solution [mM]: 145 NaCl, 4 KCl, 2 CaCl2, 1 MgCl2, 10 HEPES. pH adjusted to 7.4 with NaOH

Standard internal solution [mM]: 120 KCl, 31.25/10 KOH/EGTA, 5.374 $CaCl_2$, 1.75 $MgCl_2$, 10 HEPES. pH adjusted to 7.2 with KOH.

140 mM F- solution [mM]: 140 CsF, 1 EGTA, 5 CsOH, 10 HEPES, 10 NaCl. pH adjusted to 7.3 with CsOH.

70 mM and 28 mM F- solutions were 50:50 and 20:80 mix solutions of the standard internal solution and the 140 mM F- solution, respectively.

Sophion Bioscience A/S, Baltorpvej 154, 2750 Ballerup, Denmark
Phone: +45 4460 8800 Fax: +45 4460 8899, E-mail: info@sophion.com

sophion.com

References:

Cerne, R., Wakulchik, M., Li, B., Burris, K. D., & Priest, B. T. (2016). Optimization of a High-Throughput Assay for Calcium Channel Modulators on IonWorks Barracuda. ASSAY and Drug Development Technologies, 14(2), 75–83.

Clare JJ, Tate, SN, Nobbs, R. M. (2000). Voltage-gated sodium channels as therapeutic targets. Drug Discov Today, 5(11), 506–20.

Mccormack, K., Santos, S., Chapman, M. L., Krafte, D. S., Marron, B. E., West, C. W., … Castle, N. A. (2013). Voltage sensor interaction site for selective small molecule inhibitors of voltage-gated sodium channels. PNAS, 110(29), E2724 – 32.

Savio-Galimberti, E., Gollob, M. H., & Darbar, D. (2012). Voltage-gated sodium channels: Biophysics, pharmacology, and related channelopathies. Frontiers in Pharmacology, 3 JUL(July), 1–19.

Sun, S., Cohen, C., & Dehnhardt, C. (2014). Inhibitors of voltage-gated sodium channel Nav1.7: patent applications since 2010. Pharm Pat Anal, 5, 509–21.

Zhang, H., Reichert, E., & Cohen, A. E. (2016). Optical electrophysiology for probing function and pharmacology of voltage-gated ion channels. eLife, 5, e15202.